Supplemental Material

Cloud Phase and Relative Humidity Distributions over the Southern Ocean in Austral Summer Based on In Situ Observations and CAM5 Simulations

John J. D'Alessandro[a] and Minghui Diao

Department of Meteorology and Climate Science, San Jose State University, San Jose, California

Chenglai Wu

Department of Atmospheric Science, University of Wyoming, Laramie, Wyoming, and International Center for Climate and Environment Sciences, Institute of Atmospheric Physics, Chinese Academy of Sciences, Beijing, China

Xiaohong Liu

Department of Atmospheric Science, University of Wyoming, Laramie, Wyoming

Jorgen B. Jensen and Britton B. Stephens

National Center for Atmospheric Research, Boulder, Colorado

(Manuscript received 15 April 2018, in final form 8 February 2019)

Corresponding author: Minghui Diao, minghui.diao@sjsu.edu

DOI: 10.1175/JCLI-D-18-0232.1

[a] Current affiliation: Cooperative Institute for Mesoscale Meteorological Studies and School of Meteorology, University of Oklahoma, Norman, Oklahoma.

Table S1. Mean true air speed (m s^{-1}) at various temperature ranges for 1-s and 200-s averaged observation data.

1-s obs	Liquid	Mixed	Ice	In-cloud	Clear-sky
-10°≤T<0°C	132.9	135.2	140.0	136.2	137.7
-20°≤T<-10°C	156.0	160.6	164.2	161.9	157.1
-30°≤T<-20°C	177.5	177.4	184.2	183.1	176.7
-40°≤T<-30°C	207.6	218.1	197.2	198.2	197.7

200-s obs	Liquid	Mixed	Ice	In-cloud	Clear-sky
-10°≤T<0°C	132.2	134.7	136.6	134.2	143.0
-20°≤T<-10°C	158.4	157.4	152.6	157.3	159.0
-30°≤T<-20°C	176.3	187.6	183.1	183.1	175.7
-40°≤T<-30°C	207.7	202.9	201.8	202.3	197.0

Table S2. Number of samples (in seconds) and lengths (in kilometers) of 1-Hz observations based on the mean true air speed at various temperature ranges.

1-Hz obs	Number of samples (seconds)				Length (km)			
	Liquid	Mixed	Ice	Total	Liquid	Mixed	Ice	Total
-10°≤T<0°C	5088	1605	4904	11597	676.2	217.0	686.6	1579.8
-20°≤T<-10°C	1099	184	2954	4237	171.4	29.6	485.0	686.0
-30°≤T<-20°C	598	118	3773	4489	106.1	20.9	695.0	822.0
-40°≤T<-30°C	83	82	2463	2628	17.2	17.9	485.7	520.8
-40°≤T<0°C	6868	1989	14094	22951	970.9	285.4	2352.3	3608.6

1-Hz obs	Number of samples (seconds)			Length (km)		
	In-cloud	Clear-sky	Total	In-cloud	Clear-sky	Total
-10°≤T<0°C	11597	40255	51852	1579.8	5543.1	7128.4
-20°≤T<-10°C	4237	27955	32192	686.0	4391.7	5077.7
-30°≤T<-20°C	4489	23219	27708	822.0	4102.8	4924.7
-40°≤T<-30°C	2628	21900	24528	520.8	4329.6	4850.5
-40°≤T<0°C	22951	113329	136280	3608.6	18367.2	21981.4

Table S3. Sensitivity tests for the impacts on number and mass concentrations of cloud ice and cloud droplets due to the size range differences between observations and simulations. Results shown below are based on all the CAM-collocated model output along the ORCAS campaign. Total number of simulated samples used in this calculation is: number of columns (466163) × number of vertical levels (56) = 26,105,128 samples.

Type	Number of in-cloud samples	>30% number concentration discrepancy***	Range of Nc_{ice} discrepancy	>50% mass concentration discrepancy****	Range of IWC discrepancy
Cloud ice*	892328	494233 (0.55)	16% - 32%	21526 (0.02)	0% - 57%

Type	Number of in-cloud samples	>10% number concentration discrepancy	Range of Nc_{liq} discrepancy	>10% mass concentration discrepancy	Range of LWC discrepancy
Cloud droplet**	1006044	3694 (0.004)	0% - 29%	11160 (0.01)	0% - 33%

* Size range for cloud ice in CAM5 simulations is from 0 to infinity, while observations include 2 – 50 μm, 112.5 – 3200 μm, which means that the observations miss the size ranges of 0 – 2 μm, 50–112.5 μm, and >3200 μm.

** Size range for cloud liquid in CAM5 simulations is from 0 to infinity, while observations include 2 – 50 μm, 62.5 – 312.5 μm, which means that the observations miss the size ranges of 0 – 2 μm, 50 – 62.5 μm, and >312.15 μm.

*** Number (and fraction in parenthesis) of simulation samples that would contain >30% of cloud ice number concentrations in the missing size range that observations do not report.

**** Number (and fraction in parenthesis) of simulation samples that would contain >50% of cloud ice mass concentrations in the missing size range that observations do not report.

Table S4. Cloud phase frequency for three phases based on 5°C temperature bins.

Temperature	Obs-1s*			Korolev et al. (2017)**		
	Liquid	Mixed	Ice	Liquid	Mixed	Ice
-5°≤T<0°C	1436 (31%)	1011 (22%)	2196 (47%)	39%	24%	37%
-10°≤T<-5°C	1678 (38%)	519 (12%)	2218 (50%)	36%	16%	48%
-15°≤T<-10°C	438 (23%)	80 (4%)	1403 (73%)	18%	17%	65%
-20°≤T<-15°C	182 (12%)	96 (6%)	1427 (82%)	18%	15%	67%
-25°≤T<-20°C	172 (10%)	79 (4%)	1527 (86%)	11%	16%	73%
-30°≤T<-25°C	38 (2%)	39 (2%)	1879 (96%)	7%	13%	80%
-35°≤T<-30°C	22 (2%)	51 (5%)	903 (93%)	4%	6%	90%
-40°≤T<-35°C	40 (5%)	30 (4%)	760 (92%)	0%	5%	95%

* The in-cloud condition for Table S4 is restricted by CWC ≥ 0.01 g m^{-3} for both studies.

** Values are based on Figure 5-13 in Korolev et al. (2017).

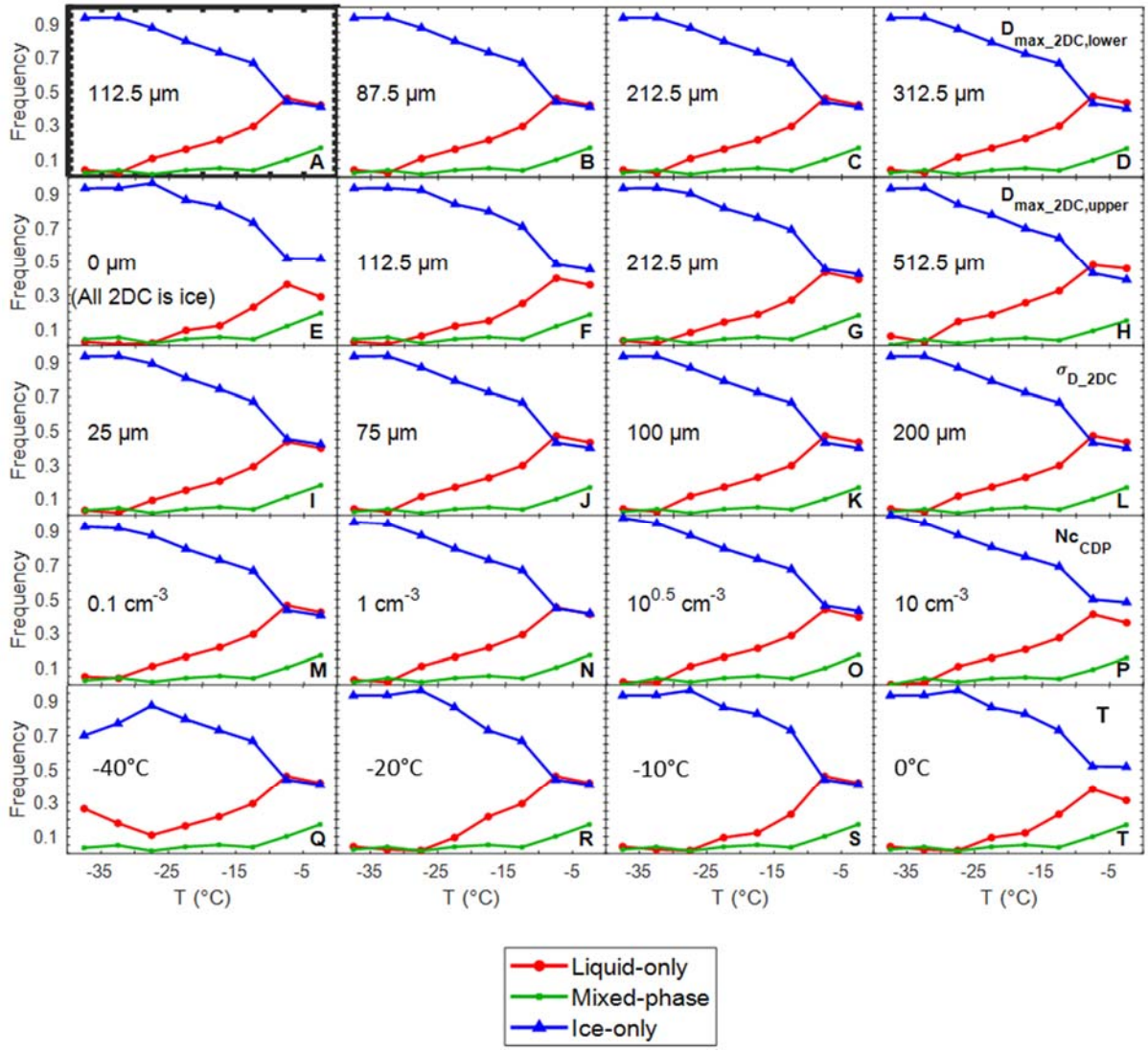

Figure S1. Sensitivity tests to the thresholds used in the cloud phase identification method. Cloud phase frequencies of liquid, ice and mixed-phase samples are shown. $D_{max\_2DC,lower}$ and $D_{max\_2DC,upper}$ thresholds represent two thresholds used for Fast-2DC data identification, with default value of 112.5 μm and 312.5 μm, respectively. That is, when $D_{max\_2DC} < D_{max\_2DC,lower}$, the data are defined as liquid droplets; when $D_{max\_2DC} > D_{max\_2DC,upper}$, the data are defined as ice; when D_{max_2DC} is between these two thresholds, further identification using σ_{D_2DC} is needed. (a) The standard method used in this work. (b-d) Testing various thresholds of $D_{max\_2DC,lower}$. (e-h) Various $D_{max\_2DC,upper}$. (i-l) Various σ_{D_2DC}. (m-p) Various Nc_{CDP}. (q-t) Various temperature thresholds used

in identifying phases in 2DC probe. The default temperature threshold is -30°C, i.e., samples are separated into < and ≥ -30°C in the method. Among all the sensitivity tests, the differences due to using various thresholds on cloud phase occurrence frequencies are less than 10%.

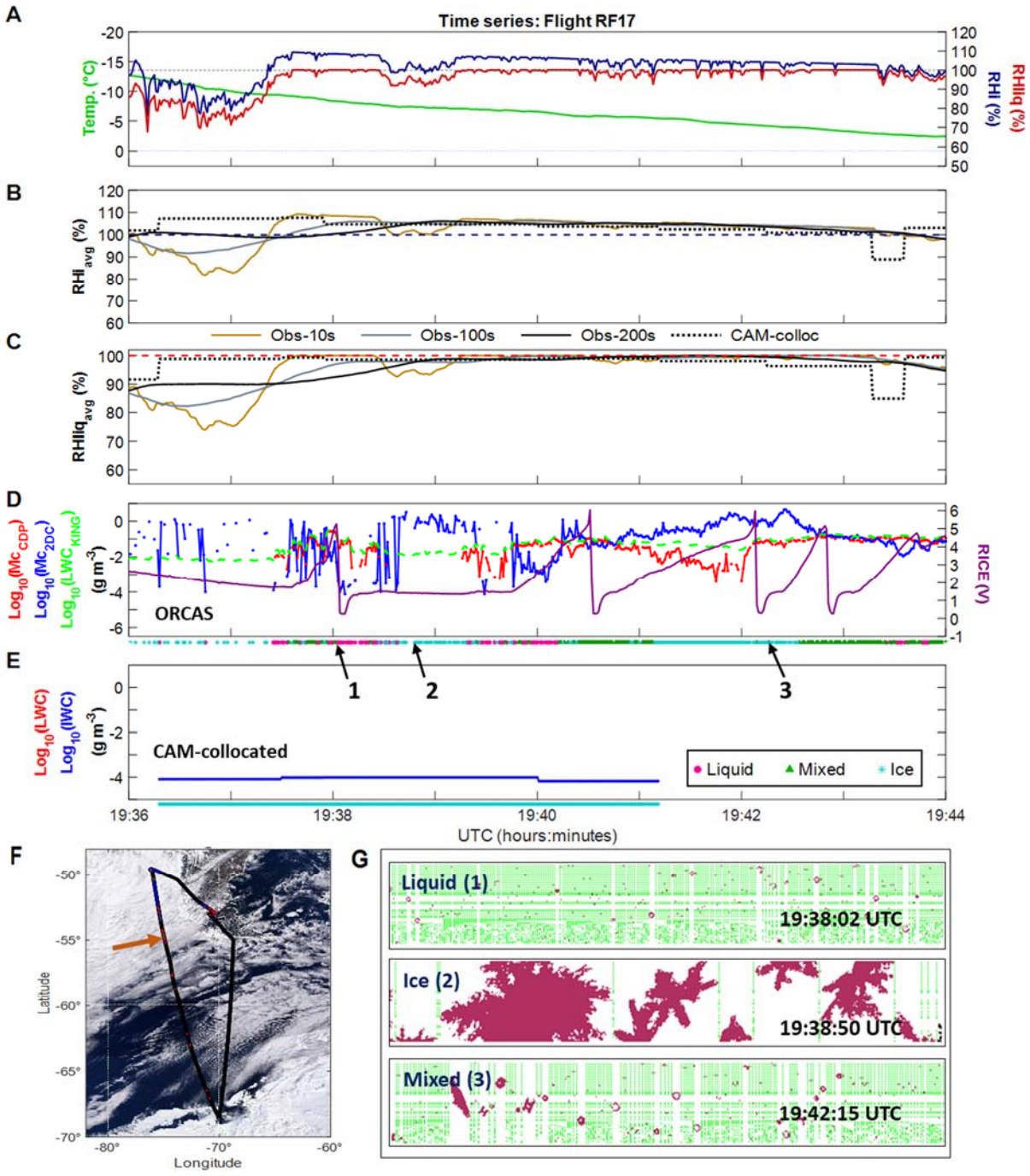

Figure S2. A time series example in RF17. All sub-panels are similar to Figure 2 in the main manuscript, except for the right axis in (D), which shows Rosemount Icing detector (RICE) measurements in voltage. The fluctuations and gradual increases of RICE voltages indicate the existence of supercooled liquid water (SLW) droplets, which agree well with the cloud phase

identification method used in this work. Note that RICE probe is not included as part of the cloud phase identification method due to its malfunction during several flights in the ORCAS campaign.

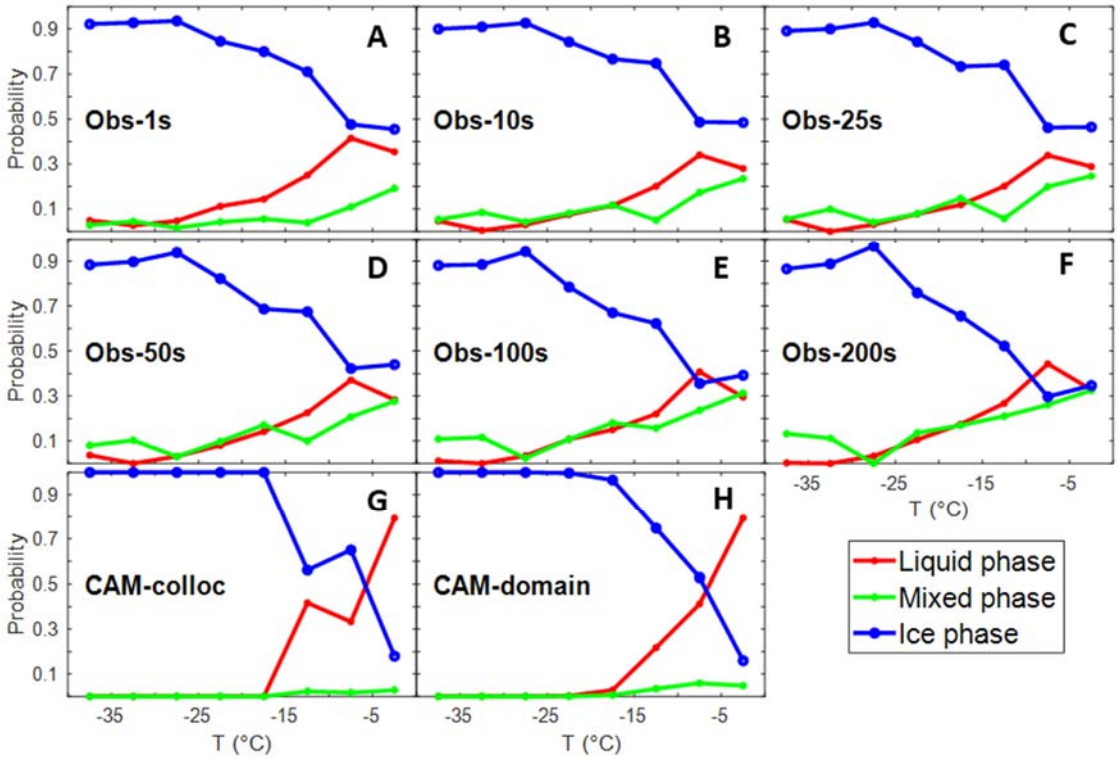

Figure S3. Cloud phase frequency of observations and simulations for the condition of cloud water content (CWC) ≥ 0.001 g m^{-3}.

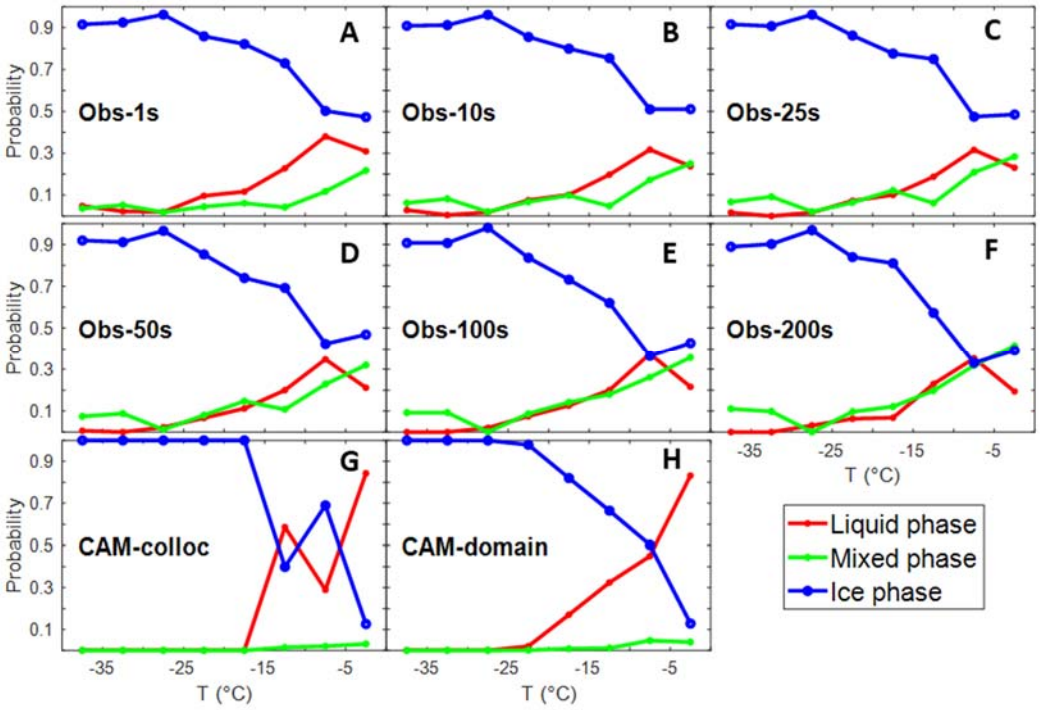

Figure S4. Similar to Figure S3, except for CWC ≥ 0.01 g m^{-3}.

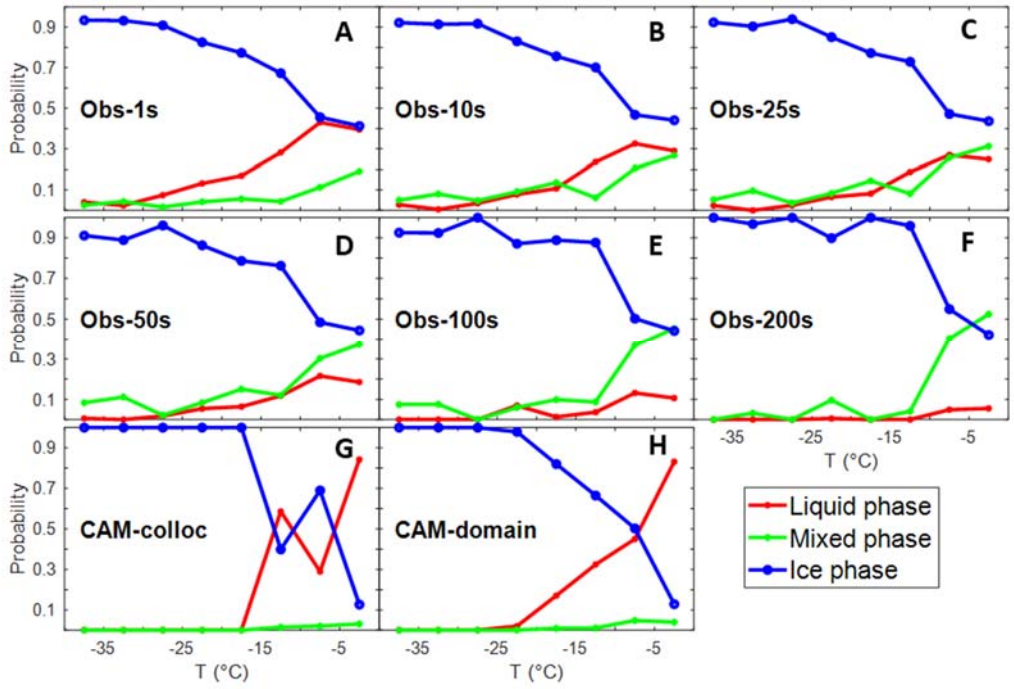

Figure S5. Similar to Figure S3, except for cloud fraction ≥ 0.6.

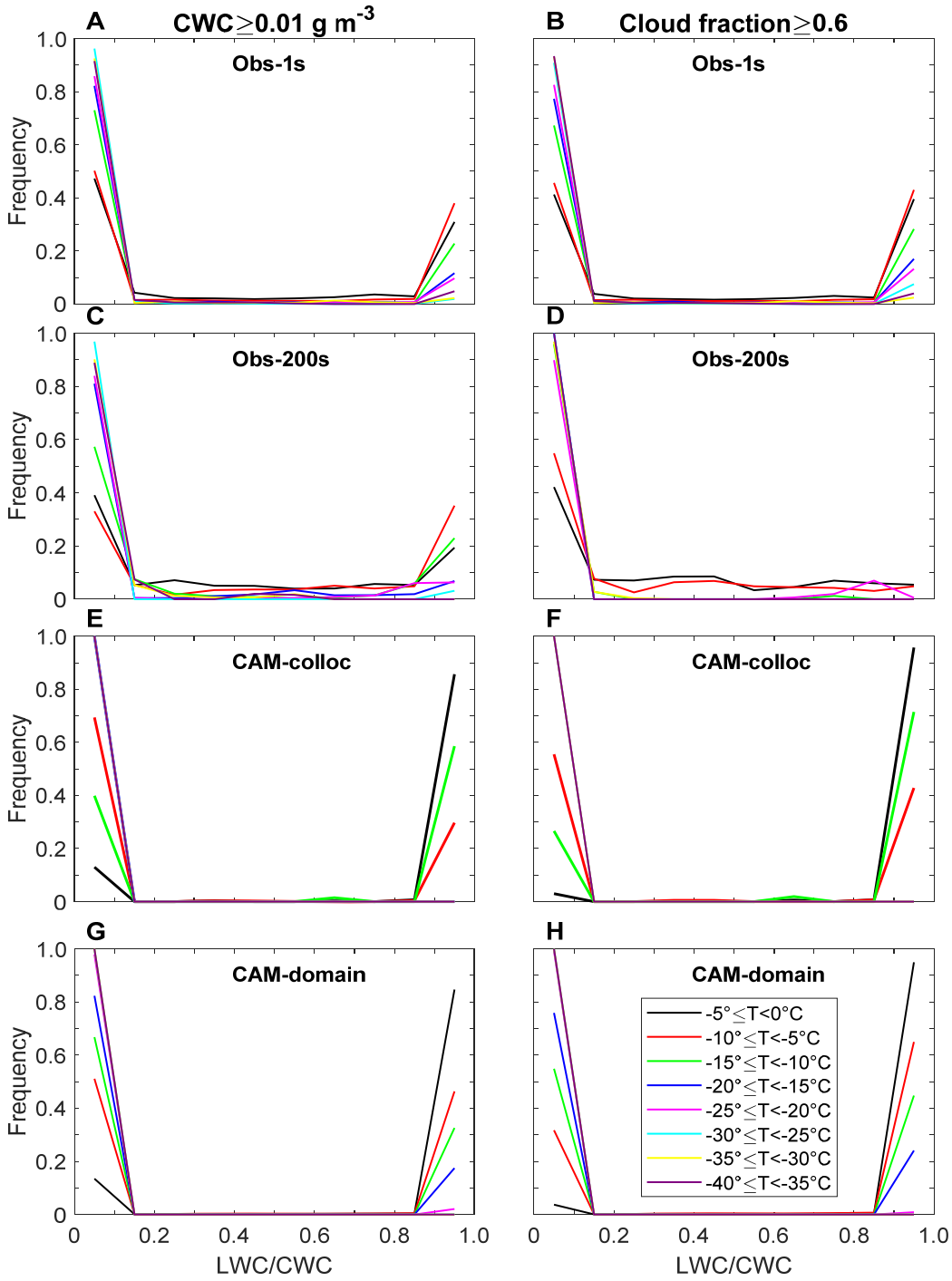

Figure S6. Cloud phase occurrence frequency for observations and simulations binned by 5°C temperature bins. This figure is similar to Figure 5 in the main manuscript, except for using a smaller temperature bin size.

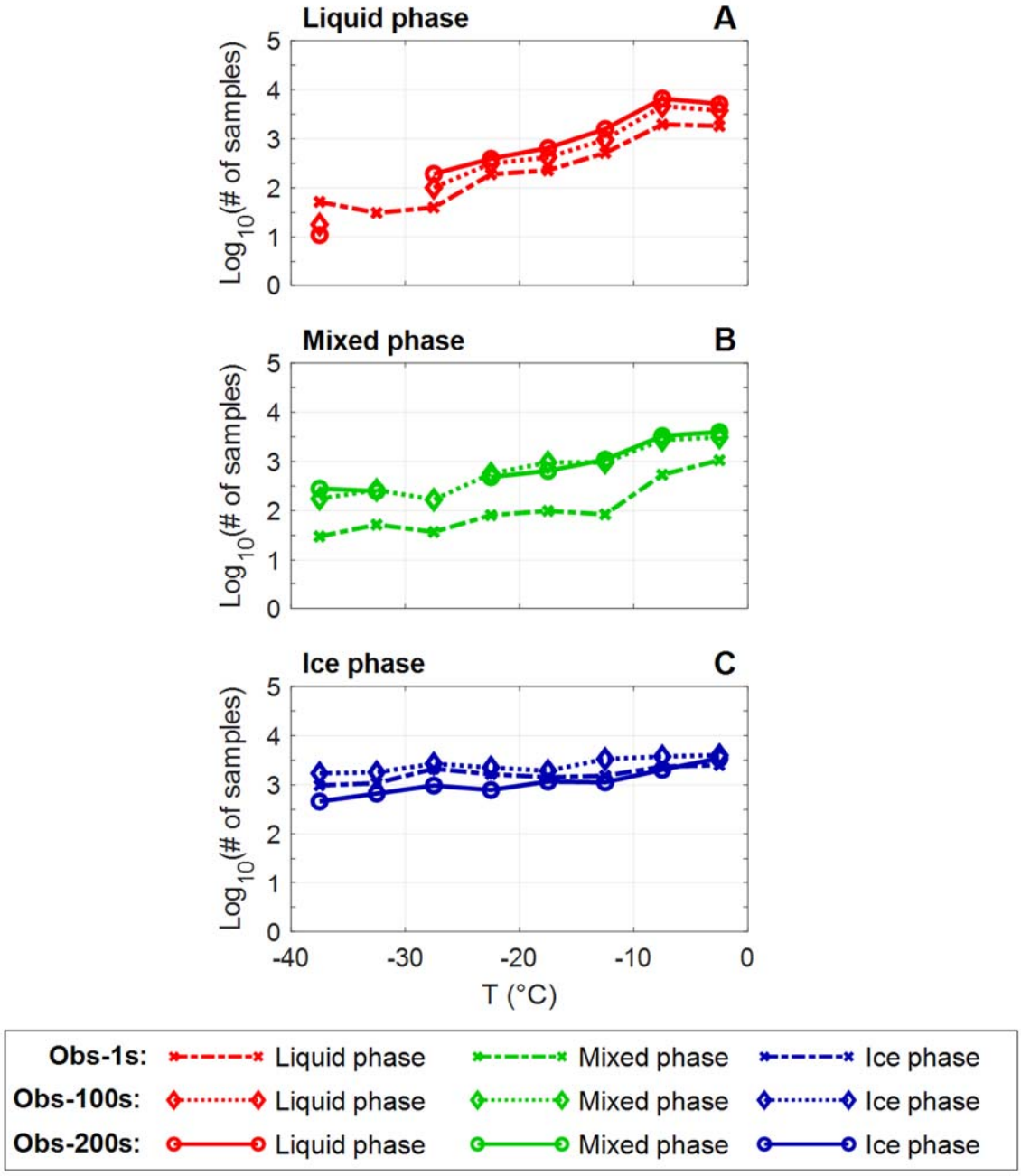

Figure S7. The number of samples for the analyses in Figure 6 in three cloud phases. The number of samples generally increases with increasing averaging scales of the analyses in Figures 6 and 7, mostly due to the restriction that a segment has to have no more than 10% reported as missing value, which is more easily satisfied by averaged data.

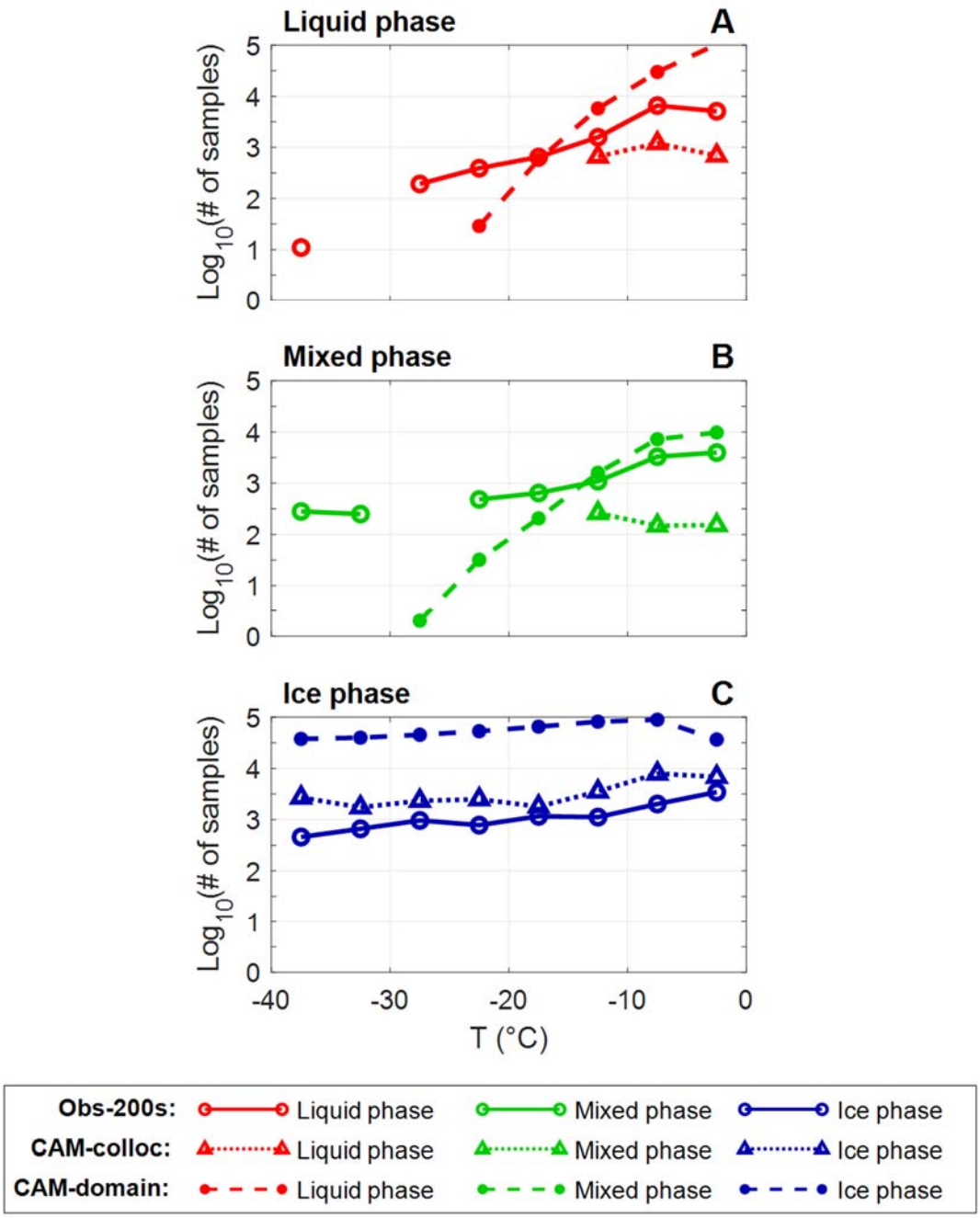

Figure S8. The number of samples for the analyses in Figure 7 in three cloud phases.

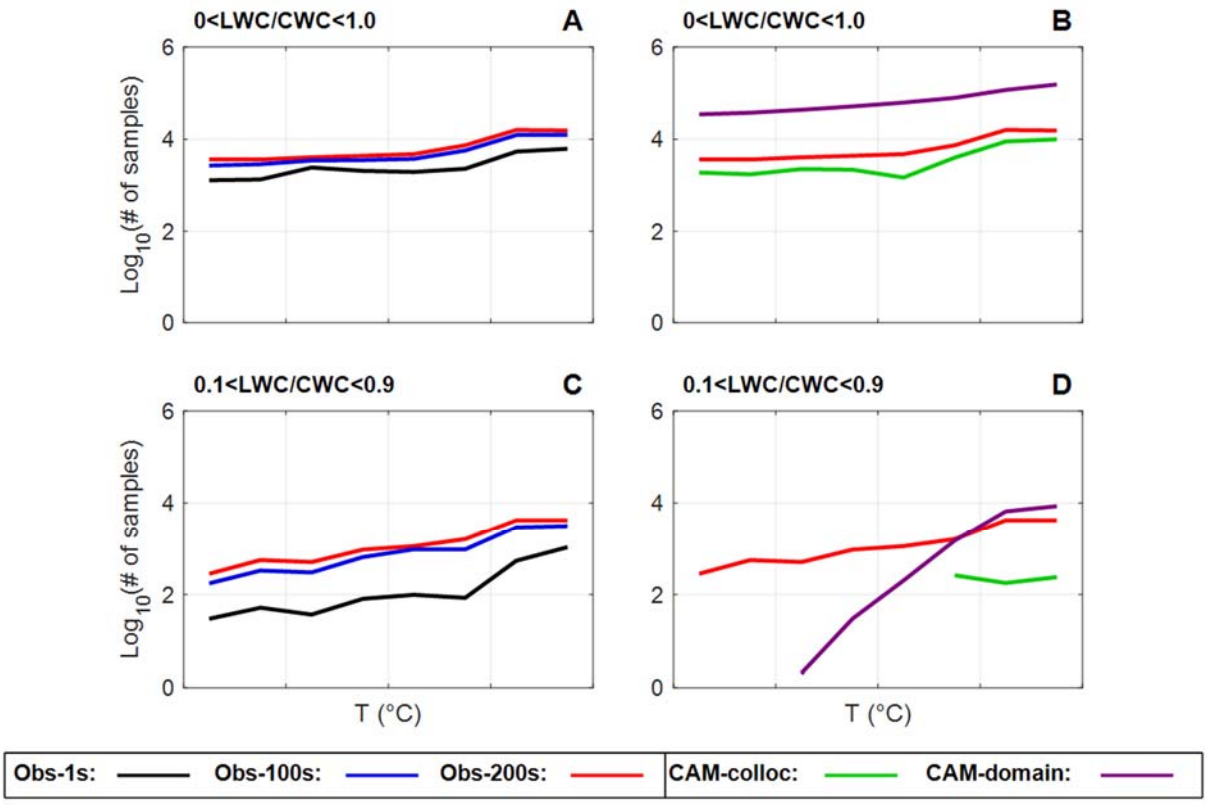

Figure S9. The number of samples for the analyses in Figure 8.

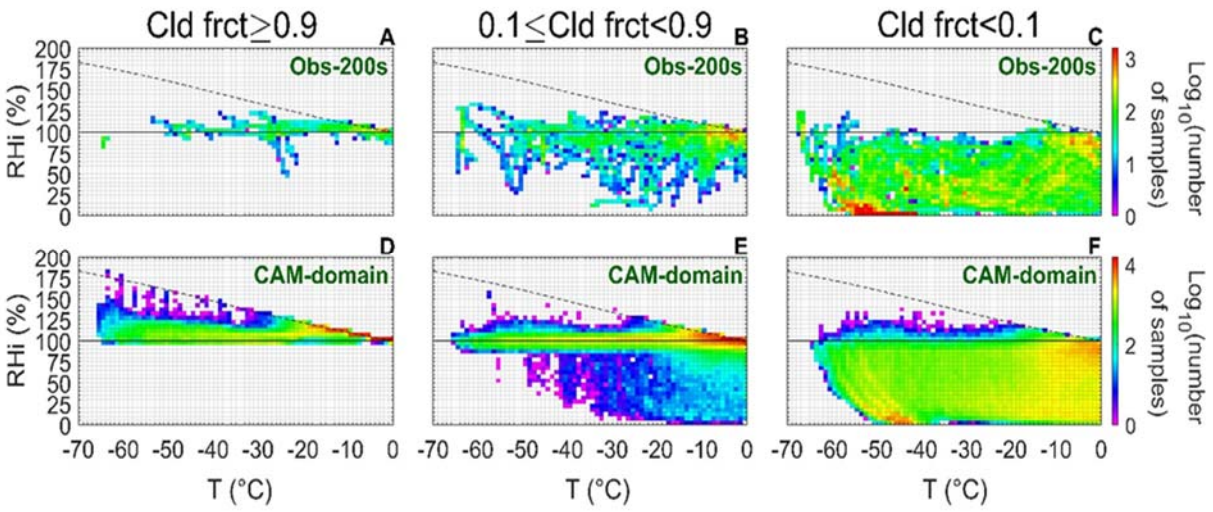

Figure S10. The number of samples for the analyses in Figure 11.

References for supplementary material:

Korolev, A., and Coauthors, 2017: Mixed-Phase Clouds: Progress and Challenges. *Meteorol. Monogr.*, **58**, 5.1-5.50, doi:10.1175/AMSMONOGRAPHS-D-17-0001.1. http://journals.ametsoc.org/doi/10.1175/AMSMONOGRAPHS-D-17-0001.1.